Real-Time Microwave Signal Processing Using Microstrip Technology

Joshua D. Schwartz[1], José Azaña[2], and David V. Plant[1]

[1]Photonics Systems Group - McGill University, Montreal, QC, H3A 2A7, Canada. [2]Institut National de la Recherche Scientifique - Énergie, Matériaux et Télécommunications, Montreal, QC, H5A 1K6, Canada

***Abstract* — We experimentally demonstrate two applications of microstrip technology in the domain of real-time microwave signal processing. Both applications employ a modulated strip width featuring a linearly distributed modulation period (i.e. linear chirp). The high-dispersion, low-loss nature of such a microstrip makes it suitable for real-time Fourier transformation, whereby an incident signal's frequency content becomes temporally ordered and can be detected or processed using time-domain methods. In addition, such a microstrip is capable of providing adjustable true-time delay by means of up- and down-conversion through conventional mixers, with potential applications for phased-array antennas.**

***Index Terms* — Microstrip circuits, signal processing, time domain measurement.**

I. INTRODUCTION

It has been recently shown that microstrips with low, uniform insertion losses, linear group delay (quadratic-phase) and high time-bandwidth products can be readily designed and manufactured [1]. By varying the strip-width of a conventional microstrip on a material with a moderate-to-high dielectric constant, an incident electromagnetic signal can be subjected to a periodic variation of impedance. When this perturbation satisfies the well-known Bragg reflection condition for an incident wavelength, that wavelength will couple to the same but counter-propagating mode at the location of the local perturbation. Such structures have come to be known as electromagnetic bandgap (EBG) devices. If, in addition, the period of the strip-width modulation is varied in a linear fashion along a length of microstrip (commonly referred to as linear chirp), different frequency components of the incident signal will experience Bragg reflection at different lengths along the device, thus the device exhibits a linear group delay.

In this work we investigate the potential of these low-loss, high dispersion devices for various microwave signal processing applications. In particular, we experimentally demonstrate (i) real-time spectral analysis and (ii) tunable true-time delay (TTD) systems based on microstrip technology. In the former application, the spectrum of a given input signal is mapped into the time-domain in real-time by propagation through a high-dispersion microstrip line; this operation would enable filtering, convolution and correlation functions of broadband microwave signals to be performed using time-domain processing [2]. In the latter application, the same microstrip is used to demonstrate a TTD system capable of adjustable delays on the order of nanoseconds, limited in bandwidth principally by the state of voltage-controlled oscillator (VCO) technology. This TTD system may prove useful in application to phased-array antennas (PAAs) and radars, which require parallel TTD elements with large enough delays to achieve full-scale angular deflection in the array.

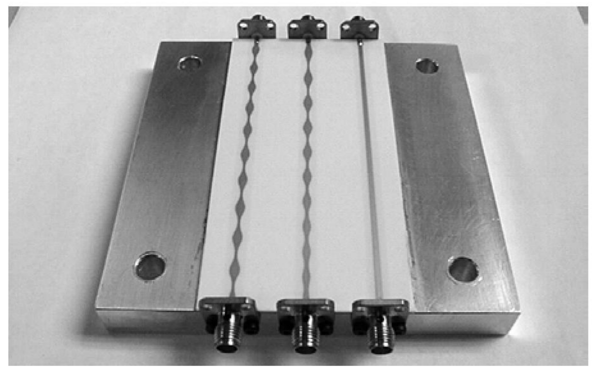

Fig. 1. Photograph of test microstrips. The center microstrip features linearly chirped width modulation.

II. TEST MICROSTRIP

For purposes of demonstrating the aforementioned applications, a test microstrip was fabricated according to the equations laid out in [1]. The strip width modulation was chosen to vary the microstrip impedance around 50 Ω from z = –L/2 to z = L/2, according to the form:

$$Z_o(z) = 50 \cdot \exp\left(A \cdot W(z) \cdot \sin\left(\frac{2\pi}{a_o} \cdot z + C \cdot \left(z^2 - \frac{L^2}{4}\right)\right)\right) \quad (1)$$

where 'C' (m^{-2}) is the chirp parameter, 'A' is dimensionless and fixes the maximum depth of modulation, 'a_o' is the central period of the device, and W(z) is a tapering function (in this case, a Gaussian) which helps to suppress long-path Fabry-Perot type resonances due to abrupt impedance transitions at the ends of the device. The general form of the impedance modulation is $\exp(\sin(\omega_o \cdot z))$ because this offers the benefits of smooth and continuous impedance variation (which reduces parasitic effects), while at the same time suppressing the harmonic resonances that would occur at multiples of ω_o with a simple sinusoid. An integration constant of $-C\cdot(L^2/4)$ is included to ensure that at each extreme of the structure (z = ±L/2) the impedance is 50 Ω-matched.

The authors' microstrip design targeted an operating bandwidth of 4 GHz with a center frequency of 6 GHz. The microstrip was 10 cm in length and was fabricated on a 1.27

0-7803-9542-5/06/$20.00

mm alumina substrate (ε_r = 9.41, tan δ = 0.0007) with gold-alloy metallization. The microstrip was mounted on an aluminum baseplate and connectorized to SMA cables (Fig 1). The design used a chirp parameter of C = -2600 m^{-2}, which corresponds to a delay slope of σ = -0.38 ns/GHz. Shown in Fig 2 are the simulated and measured S_{11} and group delay results for the microstrip, obtained respectively by Agilent's *Momentum*™ software and a vector network analyzer. The group delay features oscillations as a result of end-to-end resonances which were not completely eliminated by the applied tapering technique; however the effect of these oscillations on the overall performance is small.

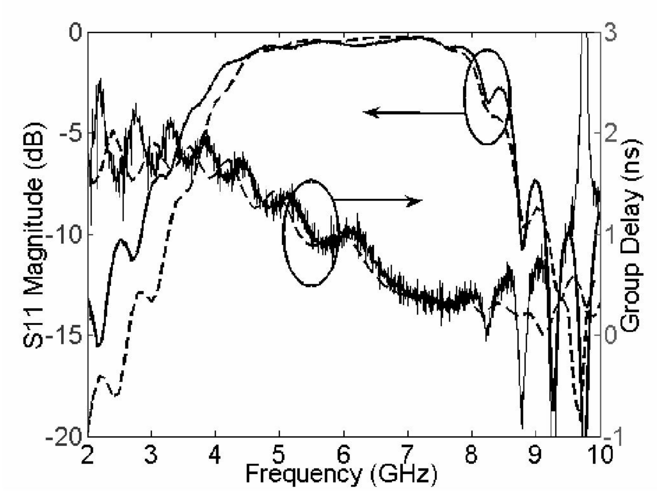

Fig. 2. Microstrip S_{11} & group delay, simulated (dash) & measured (solid)

III. Real-time Fourier Transformation

Real-time spectral analysis is a powerful signal processing tool with a myriad of interesting applications. The domain of Real-Time Fourier Transforms (RTFTs) has been explored over the years in many different kinds of media. Particular interest has been generated in mapping the spectrum of a given input signal into the time-domain in real-time; this operation would enable filtering, convolution and correlation functions to be performed using time-domain processing [2]. Such frequency-to-time mapping has already been demonstrated in optical media using dispersive fiber gratings [3]. We provide here an experimental demonstration of an RTFT based on microstrip technology.

It has been shown that a signal $s_i(t)$ constrained in time to Δt and subjected to a linear frequency-chirp with delay slope σ (ns/GHz) will decompose temporally into its FT components if the following condition is satisfied (corrected from the reference) [3]:

$$\left|\frac{\Delta t^2}{4\sigma}\right| << 1 \qquad (2)$$

In the authors' design, the condition of (2) was satisfied for signals within a time window of t << 1.2 ns, although evidence suggests that this condition can be somewhat relaxed in practice and good results can be obtained for time windows approaching 1 ns. In order to test the performance of the microstrip, a broadband 6-dB directional coupler was used to isolate the reflected response. The authors suspect that in future designs such a coupler could readily be integrated with the microstrip itself. The other end of the microstrip was 50-ohm terminated. Time-windowed test signals were generated with a high-speed pulse-pattern generator and patterns were chosen to contain frequency peaks and nulls within the frequency band of interest. It was deemed that a temporal window of 0.6 ns would be sufficient to satisfy (2). Various 6-bit patterns at frequencies of 10 and 12 Gbps (yielding spectral peaks and nulls around 5 and 6 GHz) were applied, surrounded by strings of zeros to emulate a time window. It should be noted that although the microstrip was tested here with digital bit-signaling, it is in no way limited to such signals, they were employed strictly for the experimental ease with which time-windowing could be applied.

For each input, the microstrip yielded a dispersed output signal approximately 1.5ns in length (corresponding to σ = 0.38ns/GHz over a designed bandwidth of 4 GHz). The signal contained the Fourier transform information modulated on a chirped-sinusoidal carrier frequency which varied from 4 to 8 GHz, the designed band of the microstrip. Experimental measurements were recorded using a digital sampling oscilloscope and the Fourier transform information was then extracted from the chirped sinusoid by peak-detection of the output signal (although any real-time averaging mechanism could be used instead).

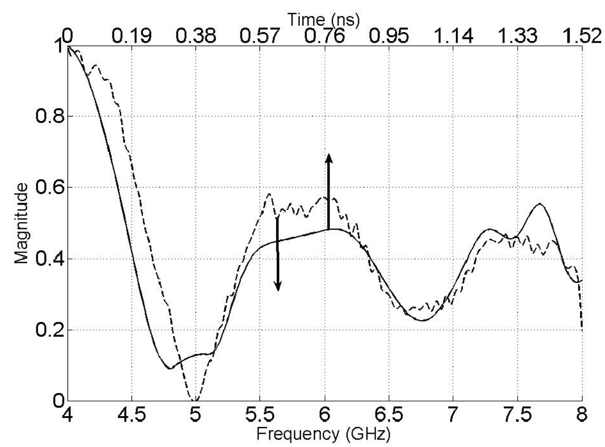

Fig. 3. The normalized spectra of 6-bit signal '100111' as measured using a spectrum analyzer (dashed, frequency domain) and a dispersive microstrip (solid, time-domain). Microstrip measurements are presented using simple peak-detected interpolation.

One example of an RTFT is presented in Fig. 3 and is directly compared to measurements taken using a conventional spectrum analyzer by scaling the time-domain detected response to the corresponding frequency range using the known dispersion slope σ of the device and the simple transformation $f = t/\sigma$. Due to the negative delay slope of the microstrip, higher frequencies were reflected first and so form the leading edge of the temporal signal, thus the signal has been reversed in time for the benefit of comparison. Some deviations, particularly near the frequency extremes, are the result of end-connector effects which would not exist in an integrated microstrip circuit. In practice, device resolution of a microstrip RTFT is limited due to the limitations of peak-detection using relatively few peaks, an effect which would be mitigated in higher-frequency bands of operation where the sinusoidal modulation yields more peaks in the temporal window of interest.

IV. TUNABLE TRUE-TIME DELAY

Tunable delay lines have received a great deal of attention for their use in a variety of applications, most notably for their application to phased-array antennas (PAAs) and radars. Interest in systems capable of true time-delay, as opposed to phase-shifters, was motivated by the desire for wideband PAAs wherein the angle of radiation was not sensitive to the frequency of the input. Since then, several schemes have been proposed for implementing tunable true time-delay (TTD) lines, including (but not limited to) signal conversion to the optical domain [4], and semiconductor and ferroelectric varactors [5], [6]. Conversion to the optical domain enables wide bandwidths of operation with fast switching times, but can involve expensive electro-optic modulation. Nonlinear delay line (NDL) approaches (e.g. varactors) can also provide very wide bandwidths and are more easily integrated, and typically provide delay variations on the order of tens of picoseconds. NDL approaches are inherently limited to operations well below the design Bragg frequency, and can be sensitive to temperature conditions.

Linearly chirped microstrips present another opportunity for a tunable TTD system implemented entirely in the electrical domain and capable in principle of adjustable delays on the order of nanoseconds with signal bandwidths limited by the state of VCO technology. The setup is shown in Fig 4, in which a pair of identical mixers is used to up-convert and down-convert an input signal to and from a frequency within the operating bandwidth of the chirped microstrip. Supposing an input centered at frequency ω_{in}, having a narrow bandwidth compared to that of the chirped microstrip, one can drive the mixers with a local oscillator (LO) such that the resulting intermediate frequency (IF), taken as the difference or sum frequency $\omega_{LO} \pm \omega_{in} = \omega_{IF}$, falls within the bandwidth of the chirped microstrip. The signal is then reflected at a particular length along the microstrip where the Bragg condition is satisfied. The reflected signal passes to the second mixer, restoring the signal to its original frequency (neglecting, for the moment, the issue of image-frequency filtering). By tuning ω_{LO} (for example, with a high-power VCO) one can cause the signal to travel different path lengths into the microstrip before experiencing reflection; thus the chirped microstrip enables a tunable time-of-flight delay.

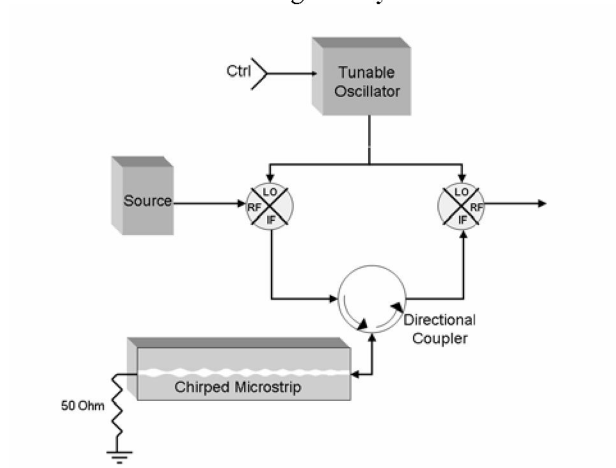

Fig. 4. TTD block diagram.

The maximum possible variation in time delay $\Delta\tau$ introduced by this mechanism is controlled by the length of the microstrip and the effective permittivity of the medium according to the following:

$$\Delta\tau = \frac{2L\sqrt{\varepsilon_{eff}}}{c} \tag{3}$$

Microstrip length, bandwidth of operation, and delay slope are intimately related. For a given microstrip length, higher bandwidths of operation require lower delay slopes. In general, the microstrip bandwidth should be designed in accordance with the bandwidths of the available VCO in the system, as this will typically be the limiting factor. The speed at which the full-scale delay may be scanned is limited by the state-of-the-art in VCO technology. An example VCO (*Herley's* V6040) capable of supplying +10 dBm of LO power over a bandwidth of 4 GHz has a switching speed on the order of 50 ns. Some restriction on the bandwidth of the input signals is necessary to avoid dispersion-induced distortion of the signal. Overall system attenuation of the signal will be dominated by the conversion loss of the mixers. Active mixing or amplification may be employed to compensate for system losses. Insertion losses incurred by the microstrip itself are minimal (the authors achieved an S_{11} of about -1 dB within the operating band with ease). In addition, proper filtering must be added to ensure image-frequency rejection.

For this scheme to be employed in a parallel manner (e.g. for a PAA with many elements), system size would be dominated by the length of the microstrip, for which a typical structure can be on the order of several centimeters. This can be mitigated by raising the frequency of operation of the microstrip, resulting in shorter structures. Such structures will exhibit higher losses (in proportion to $\sqrt{\omega}$), however a judicious use of tapering techniques and asymmetric windowing applied to the microstrip modulation can raise the reflectivity of higher frequencies and remove undesired harmonics [1]. Tapering techniques also improve the linearity of the microstrip group delay by reducing long-path resonances that cause group delay ripple.

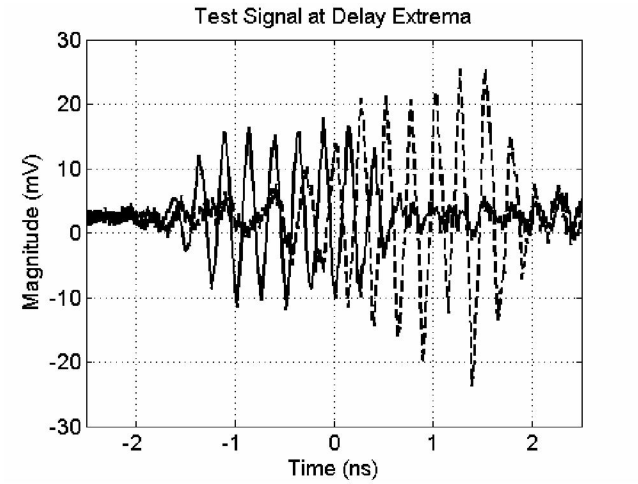

Fig. 5. Example of signal output at the full-scale delay extrema for an input signal centered at 4 GHz. 1.5 ns delay (dash) is demonstrated as compared to a reference (solid).

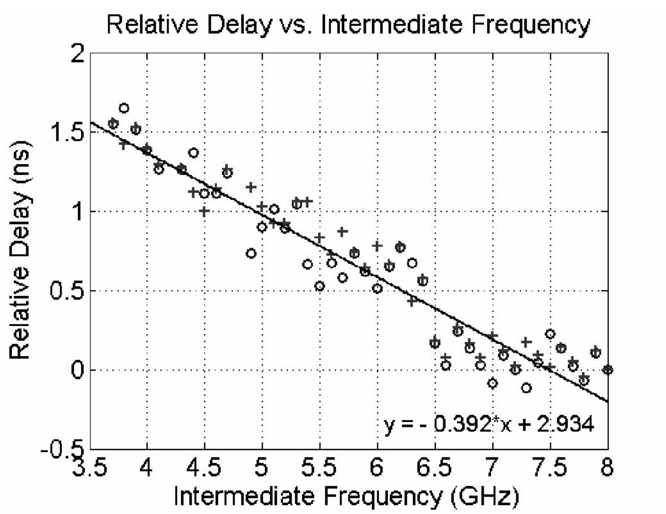

Fig. 6. Measured relative delay introduced into a bit sequence by tuning the local oscillator. Two data sets (o) and (+) are shown for two identical test microstrips, along with a linearization of (o) indicating delay slope.

A simple proof-of-concept demonstration was carried out using the previously introduced microstrip. The microstrip features an effective permittivity of ε_{eff} = 6.34 for a corresponding delay range, according to (3), of $\Delta\tau$ = 1.68 ns. Employing commercially available mixers and a synthesized local oscillator, a 16-bit alternating sequence was used to approximate a short, narrow-band signal centered at 4 GHz. The LO was tuned between 7.5 GHz and 12 GHz, resulting in IF values in range of the microstrip. Experimentally measured output signals from the TTD system are shown in Fig. 5, demonstrating the full-scale delay of approximately 1.5 ns, in agreement with the prediction. Some variation in signal attenuation was observed over the range of delay values, attributable to frequency-dependent mixer conversion loss and directional coupling, neither of which were optimized. Plots of measured signal delay recorded for two identical test microstrips are shown in Fig. 6 and demonstrate that a delay slope of approximately -0.39 ns/GHz was achieved in the device, with some anticipated ripple based on the group delay in Fig. 2.

V. Conclusion

Low-loss, high-dispersion filters based on microstrip technology have been fabricated and demonstrated for implementing two different operations of practical significance, namely real-time spectral analysis, and adjustable true time-delay. These results demonstrate the potential of chirped microstrips for a myriad of analog signal processing applications, such as real-time filtering, convolution and correlation functions of broadband microwave signals, as well as potential applications in phased-array antennas and radars.

Acknowledgements

The authors gratefully acknowledge the support of Mr. Robert Morawski and Professor Tho le-Ngoc for their experimental assistance.

References

[1] M. A. G. Laso, T. Lopetegi, M. J. Erro, D. Benito, M. J. Garde, M. A. Muriel, M. Sorolla, and M. Guglielmi, "Chirped delay lines in microstrip technology", IEEE Microwave. Wireless Comp. Lett. (USA), vol. 11, pp.486-488, Dec. 2001.

[2] M. A. G. Laso, *et al.* "Real-time spectrum analysis in microstrip technology", IEEE Trans. Microwave Theory Tech., vol. 51, pp.705-717, Mar. 2003.

[3] J. Azaña, L. R. Chen, M. A. Muriel and P. W. E. Smith, "Experimental demonstration of real-time Fourier transformation using linearly chirped fiber bragg gratings", Electron. Lett. , vol 35, pp.2223-2224, Dec. 1999.

[4] J. L. Corral, J. Marti, J. M. Fuster, and R. I. Laming, "True time-delay scheme for feeding optically controlled phased-array antennas using chirped-fiber gratings," *IEEE Photon. Tech. Lett.*, vol. 9, pp.1529-1531, Nov. 1997.

[5] C. Chang, C. Liang, R. Hsia, C. W. Domier, and N. C. Luhmann Jr., "True time phased antenna array systems based on nonlinear delay line technology," in *Proc. Asia-Pacific Microwave Conf.*, Taipei, Taiwan, R.O.C., Nov. 2001, pp. 795-799.

[6] D. Kuylenstierna, A. Vorobiev, P. Linnér ,and S. Gevorgian, "Ultrawide-band tunable true-time delay lines using ferroelectric varactors," *IEEE Transactions on Microwave Theory and Tech.*, vol. 53, pp.2164-2170, Jun. 2005.